Fragmentation of ^{28}Si nuclei in nuclear emulsion

M El-Nadi†, M S El-Nagdy‡, N Ali-Mossa§, A Abdelsalam†, A M Abdalla§ and A A Hamed‖

† Physics Department, Faculty of Science, Cairo University, Cairo, Egypt
‡ Physics Department, Faculty of Science, Helwan University, Ain Helwan, Cairo, Egypt
§ Basic Science Department, Faculty of Engineering, Zagazig University, Benha Branch, Egypt
‖ National Center for Nuclear Safety and Radiation Control, AEA, Cairo, Egypt

Abstract.   Topology of ^{28}Si fragmentation at 14.6 A GeV in emulsion nuclei is given. In all events, the charge of each projectile fragment is measured. We report the measurements on total and some partial reactions cross sections of ^{28}Si interactions. The data for $Z \geqslant 6$ can be qualitatively described by a statistical percolation model. The results are discussed and compared with those obtained from ^{28}Si at 3.7 A GeV and ^{32}S at 200 A GeV.

1. Introduction

Relativistic heavy-ion collisions have been regarded as promising for giving information about the underlying production processes. The number of participant nucleons in these collisions is very important for the study of meson production [1] and resonance matter. It also serves as an experimentally accessible substitute for the impact parameter. The expression 'participant nucleons' stems from the participant–spectator model in which nucleons residing in the geometrical overlap between projectile and target are considered participants of the heavy-ion collision, whereas the nucleons not residing in the overlap are termed spectators.

Nuclear emulsion has the highest (4π) spatial resolution compared with any other detector. Moreover, in emulsion not only the projectile fragments (PF) can be detected but also all the target fragments, which helps in the analysis of the events.

In this paper we focus on multiplicity distributions of fragments, charged secondaries, and their dependence on incident energy. The topological structure of the projectile fragmentation of ^{28}Si nuclei at 14.6 A GeV is studied. It was first discussed by the EMU01 collaboration [2] for the fragmentation of ^{28}Si at 3.7 A and 14.6 A GeV, and ^{32}S at 200 A GeV. An attempt is made to compare their results with ours. Such a comparison may provide additional information helpful to understanding the fragmentation process.

2. Experimental set-up and methods of measurements

Beams of ^{28}Si were accelerated to 14.6 A GeV at Brookhaven National Laboratory (BNL) Alternating Gradient Synchroton (AGS). A nuclear photoemulsion stack of FUJI type was horizontally exposed to the ^{28}Si beam. The dimensions of the emulsion pellicles were $16 \, \text{cm} \times 10 \, \text{cm} \times 600 \, \mu\text{m}$. The stack was exposed to a total of about 2.4×10^4 ions in the centre of the stack. The flux intensity was 3×10^3 particles cm^{-2}. The grain density for a minimum

ionizing particle is about 30 grains per 100 μm. The interactions were found by double-scanning along the track, fast in the forward direction and slow in the backward direction. The pellicles were scanned on a STEINDORFF microscope under high magnification $100\times$ using oil immersion objectives. The primary tracks were picked up at the entering edge of the pellicles and were carefully followed until they either interacted or escaped from the pellicle. Events due to elastic scattering are excluded. In a total length of 121.77 m of the scanned tracks, 962 events were attributed to inelastic interactions of ^{28}Si projectile with emulsion nuclei, leading to an experimental mean free path $\lambda_{\text{exp}} = 12.65 \pm 0.42$ cm, corresponding to an experimental cross section of $\sigma_{\text{exp}} = 1000 \pm 40$ mb. For each detected interaction, the following characteristics features were recorded: N_s, the number of minimum ionizing shower tracks with kinetic energy $E > 400$ MeV and very high velocity $\beta = v/c \geqslant 0.7$ (most N_s tracks are π-mesons); N_g, the number of grey tracks (recoil protons with $40 < E < 400$ MeV, $0.3 < \beta < 0.7$ and range $R > 3$ mm and N_b, the number of black tracks due to evaporated target fragments with $E < 40$ A MeV, $\beta \leqslant 0.3$, $R \leqslant 3$ mm. $N_g + N_b$ is the sum of heavily ionizing charged particles, denoted by N_h.

The nuclear emulsion used here contains hydrogen (16.80%), carbon (15.15%), nitrogen (3.66%), oxygen (11.57%), sulfur (0.22%), bromine (24.28%), silver (28.14%) and iodine (0.17%). The percentage given for each element is the reaction percentage of ^{28}Si (14.6 A GeV) induced reactions. The number N_h emitted in an interaction is an important parameter and greatly helps in separating events due to target types, i.e., all events due to H interactions have $N_h = 0, 1$. The interactions having $N_h \geqslant 8$ almost definitely belong to AgBr collisions, while events with $N_h \leqslant 7$ are due to interactions with CNO and AgBr. To separate the experimental events corresponding to each group, we draw the integral frequency distribution of events as a function of N_h for all inelastic interactions of ^{28}Si with different emulsion targets. Further details of the experimental separation and identification of events are given in [3, 4]. It was found that the events due to H, CNO and AgBr were estimated to be 111 (15.3%), 224 (30.8%) and 392 (53.9%), respectively.

In each event, the PF representing the projectile-like (non-interacting) fragments with a charge $Z \geqslant 2$ are also recorded where the charge of each of these PF is identified by its grain density, by its gap-length distribution, or by its δ-ray density measurements [5]. On the other hand, at each interaction point, the PF with $Z = 1$ can be well separated. These PF correspond to a spectator proton with a transverse momentum of 14.6 MeV/c. All PF are emitted within the fragmentation cone defined by a critical angle $\theta_c = P_f/P_{\text{beam}}$, where, P_{beam} stands for the beam momentum and P_f for Fermi momentum ($\sim$160 MeV/c) [6]. For the ^{28}Si ions at 14.6 A GeV, $\theta_c \sim 12$ mrad.

As shown in figure 1, each track length followed for a δ-ray count was >1.0 cm. In order to measure the charge of each projectile fragment, a calibration curve is constructed by using δ-ray of primary ^{28}Si beams and He PF, chosen as charge references. As for He PF, it is easily identified in all labs. The confusion between the He PF and other PF with $Z = 3$ or 4 has only a small effect due to the rare production of these latter fragments.

Using the proportionality of the number of δ-ray per mm (N_δ) with Z^2 of the fragment, i.e., $\frac{N_\delta \text{ for } ^{28}\text{Si}}{N_\delta \text{ for } ^4\text{He}} = \frac{Z_{\text{Si}}^2}{Z_{\text{He}}^2}$ one is able to obtain the linear relation expressed by $N_\delta = A + BZ^2$ where $A = 0.136$ and $B = 0.169$. This equation is verified by checking the charge conservation [7] characterizing the electromagnetic dissociation events having either only one heavy PF (i.e., $\text{Si}_{14} \rightarrow \text{Si}_{14}$) or only one heavy PF accompanied by the emission of α-particles (e.g., $\text{Si}_{14} \rightarrow \text{Mg}_{12} + \text{He}_2$ or $\text{Si}_{14} \rightarrow \text{Ne}_{10} + 2\text{He}_2$) where it is found that the present accuracy of the charge identification is less than ± 1 unit. Here, we obtain the δ-ray per mm distribution (figure 1) for PF having charge $Z = 2$–14 emitted from a ^{28}Si projectile by following each
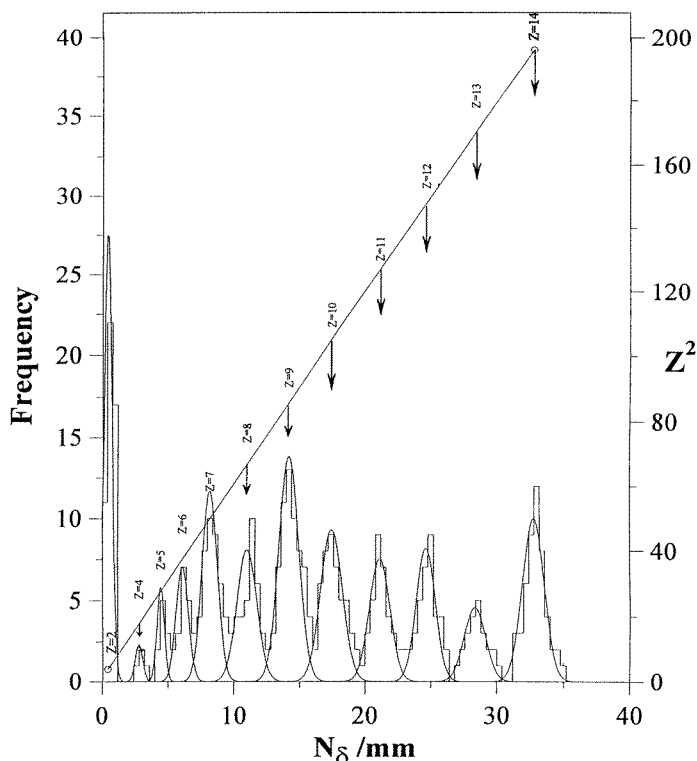
Figure 1. The calibration curve (Z^2 versus N_δ mm^{-1}) for relativistic ^{28}Si and ^{4}He tracks (on the right). The frequency distribution (histogram) of the relativistic PF as a function of N_δ mm^{-1}. Each curve represents the Gaussian distribution corresponding to each fragment. The position of the arrow for each charge has been determined according to the peak of the corresponding distribution (on the left).

track for at least 1 cm track length. The $Z = 2$ histogram represents the δ-ray measurements for 50 tracks produced in a randomly chosen inelastic interaction. On the other hand, the $Z = 14$ histogram indicates the results of the measurements for a sample of 35 tracks of ^{28}Si beam in addition to 15 projectile tracks having $Z = 14$. A series of histograms were observed. Each of these histograms can be fitted by a Gaussian distribution with a peak corresponding to a certain value of Z, which can be determined by using the calibration line as illustrated by the associated arrow.

3. Results

With the above-mentioned criteria for separation and identification of the PF we obtain the topology given in table 1. In figure 2 we show the topology for all events of the minimum biased sample obtained from this work (i.e., events with $N_h \geqslant 0$) in comparison with the corresponding ones [2] for 3.7 A GeV ^{28}Si and 200 A GeV ^{32}S. It should be noticed that the distribution emanating from ^{32}S fragmentation is normalized to the ^{28}Si yield for all channels with $Z \leqslant 14$, i.e., we eliminate the two highest values of $Z = 15$ and 16 from the ^{32}S spectrum.

It should be noticed that figure 2 includes the results of some channels observed in [2] which are not detected in this work.

Table 1. Topology of the ^{28}Si fragmentation at 14.6 A GeV (minimum bias).

Channels	N_h			
	0–1	2–7	$\geqslant 8$	$\geqslant 0$
Si	15	—	—	15
Al + H	13	6	4	23
Mg + He	3	4	—	7
Mg + 2H	10	14	5	29
Na + He + H	4	3	2	9
Na + 3H	2	18	7	27
Ne + 2He	3	2	—	5
Ne + He + 2H	9	12	5	26
Ne + 4H	3	10	3	16
F + 2He + H	3	7	—	10
F + He + 3H	8	19	5	32
F + 5H	3	12	6	21
O + Be + 2H	—	—	1	1
O + 2He + 2H	2	7	3	12
O + He + 4H	6	7	3	16
O + 6H	1	6	1	8
N + C	—	1	—	1
N + 3He + H	—	2	—	2
N + 2He + 3H	6	5	4	15
N + He + 5H	6	5	5	16
N + 7H	3	3	1	7
C + B + He + H	1	1	—	2
C + 3He + 2H	1	1	—	2
C + 2He + 4H	3	3	3	9
C + He + 6H	—	7	—	7
B + 4He + H	1	—	—	1
B + 2He + 5H	2	2	1	5
B + He + 7H	1	1	1	3
B + 9H	—	1	—	1
Be + 4He + 2H	1	—	—	1
Be + 3He + 4H	1	1	—	2
Be + 2He + 6H	1	—	—	1
6He + 2H	—	1	—	1
5He + 4H	4	6	—	10
4He + 6H	6	5	2	13
3He + 8H	8	18	15	41
2He + 10H	17	19	38	74
He + 12H	14	38	62	114
14H	—	24	89	113
0^a	—	1	28	29
All	161	272	295	727

^{a} No fragments of projectile in a narrow forward one (i.e., $Q = 0$).

The topology seen in table 1 represents all minimum biased events in which each channel includes the participants and the spectators of the Si beam. The participant part is represented by some or all of the H-fragments, so that the total charge in each channel should be 14. The N + C channel is represented twice: once for N+ anything and once for C+ anything. Figure 2, on the other hand, represents the charge distribution (spectators) of the Si beam with and without He PF in comparison with the corresponding data of ^{28}Si(3.7 A GeV) and
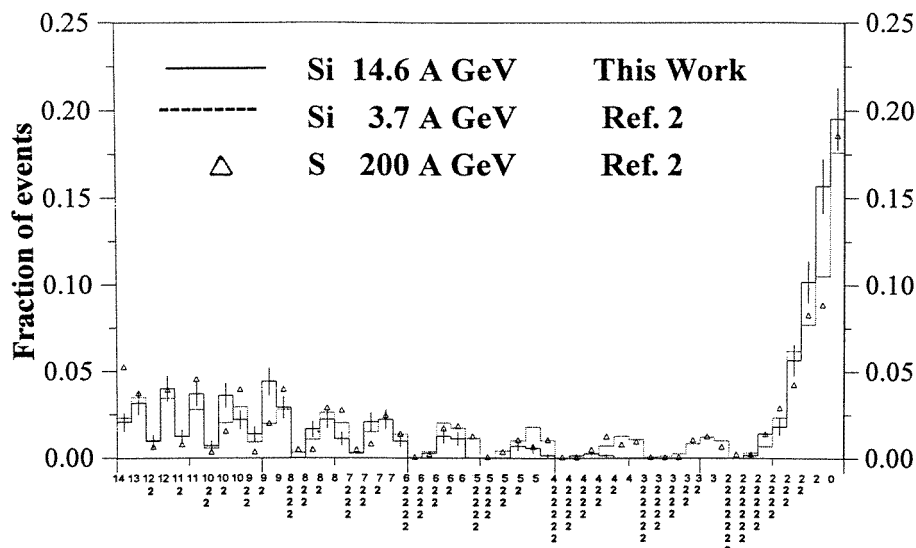
Figure 2. Topological diagram for $N_h \geqslant 0$ events. The numbers below the x-axis represent the charge distribution of the spectators with and without α-fragments.

^{32}S(200 A GeV) taken from [2].

The similarity of the three distributions obviously indicates that the beam energy is of little importance for the nuclear fragmentation process except probably for the most peripheral interactions. The yields of multiply charged fragments are the same at 3.7, 14.6 and 200 A GeV, except for the region of $Z = 3$–6 where the present yield is lower than the corresponding one of Adamovich *et al* [2]. This may be due to shell effects [8] in which it is assumed that all fragments with masses 5, 8 and 9 decay into α-particles and protons. However, evidence for a limited fragmentation hypothesis is shown which implies that both projectile and target may be fragmented irrespective of each other, and that this fragmentation is dependent on the beam energy.

The event statistics for the two samples given by EMU01 collaboration [2] and that obtained from this work are given in table 2. This table also shows the number of events with total projectile destruction (TD). TD events are defined as those events where only PF with charge $Z \leqslant 2$ remain. The ratio between the number of collisions having $2 \leqslant N_h \leqslant 7$ (CNO and peripheral AgBr) and the number of collisions having $N_h \geqslant 8$ (only AgBr) is independent of the beam energy.

[9] shows that the cross section of TD events should follow a geometrical formula like the one predicted by Bradt and Peters [10] for relativistic (inelastic) nucleus–nucleus interactions. Accordingly, Adamovich *et al* [2], parametrized their results in terms of cross section such that:

$$\sigma_{TD} = (1.58 A_1^{0.026})^2 (A_1^{1/3} + A_2^{1/3} - 0.85 A_1^{0.38})^2 \text{fm}^2 \tag{1}$$

where A_1 and A_2 denote the mass numbers of the projectile and target, respectively. Table 3 gives a comparison between the experimental and calculated values. Events with $N_h = 0, 1$ are predominately 'quasi-nucleon' interactions, i.e., interactions with a H-nucleus or with only one bond nucleon in CNO or AgBr. The $N_h = 2$–7 group is dominated by CNO collisions and peripheral AgBr collisions whereas the $N_h \geqslant 8$ group consists of AgBr interactions with a substantial degree of disintegration. This table shows that, within the margin of error, there is an

Table 2. The statistics of events for 37 and 14.6 A GeV ^{28}Si compared with 200 A GeV ^{32}S interactions with emulsion for different N_h groups.

		Projectile		
		^{28}Si (14.6 A GeV)		
	^{28}Si (3.7 A GeV) [2]	This work	[2]	^{32}S (200 A GeV) [2]
Total number of collisions	1986	727	995	775
$N_h = 0, 1$	443	161	265	283
$2 \leqslant N_h \leqslant 7$	734	272	328	234
$N_h \geqslant 8$	809	295	362	258
$N(2 \leqslant N_h \leqslant 7)/N(N_h \geqslant 8)$	0.91 ± 0.07	0.92 ± 0.08	0.91 ± 0.09	0.91 ± 0.12
Events with total destruction of the projectile nucleus with $(Z \leqslant 2)$				
$N_h = 0, 1$	75	49	58	50
$2 \leqslant N_h \leqslant 7$	265	112	135	80
$N_h \geqslant 8$	557	234	273	166
$N(2 \leqslant H_h \leqslant 7)/N(N_h \geqslant 8)$	0.48 ± 0.05	0.48 ± 0.06	0.49 ± 0.07	0.48 ± 0.09

Table 3. Percentages of TD events in ^{28}Si–Em interactions at 14.6 A GeV with various degrees of target break-up. The calculations are based on equation (1).

N_h range	Exp.	Calc.
0,1	30 ± 5	35
2–7	41 ± 5	47
$\geqslant 8$	79 ± 7	76

agreement, for each range of N_h, between the fraction of the TD events and the corresponding calculations. This agreement was also observed in [2] for ^{28}Si at 3.7 A and 14.6 A GeV and for ^{32}S at 200 A GeV, from which we can conclude that the yield of total destruction of events is energy independent within range 4–200 A GeV.

In the second group of events, i.e. those having fragments with $Z \geqslant 3$, it is noticed that there is some energy dependence, particularly in the channels with a small degree of disintegration. This mainly comes from the quasi-nucleon ($N_h = 0, 1$) events. Figure 3 represents the average charge ($\langle n(Z) \rangle$) and multiplicity distributions of fragments in interactions of quasi-nucleon-type events compared with that predicted according to the bond-percolation prescription [2, 11, 12] in which the nucleus is considered as a cubic lattice where each nucleon has bonds to its nearest neighbours. Only one parameter P, the probability of breaking a bond, is introduced after the dimension of the lattice is set. The authors in [2] have shown that for ^{28}Si the cubic $3 \times 3 \times 3$ lattice is a good approximation. The calculated mass distribution is transformed into a charge distribution by the assumption that all $A = 3, 4$ isotopes correspond to $Z = 2$, $A = 5, 6$ isotopes to $Z = 3 \ldots$ etc. In figure 3 such calculations are illustrated for $P = 0.55$ and $P = 0.60$. The present yield of $Z = 2$ fragments has been normalized to the corresponding one at 3.7 A GeV [2]. The normalized fraction thus obtained was used for obtaining the total distribution. One can see that the calculations of [2] (where these calculations are normalized to fit the region $Z = 6$–9) reproduce the experimental multiplicity distributions (figure 3(*b*)) and the charge distributions for $Z \geqslant 5$. Also the rise for $Z = 2$ is predicted but the details of Z dependence in the region $2 \leqslant Z \leqslant 5$ is not well described.

The critical value [2] of P is about 0.75 and hence the best fit for $P = 0.60$ indicates that
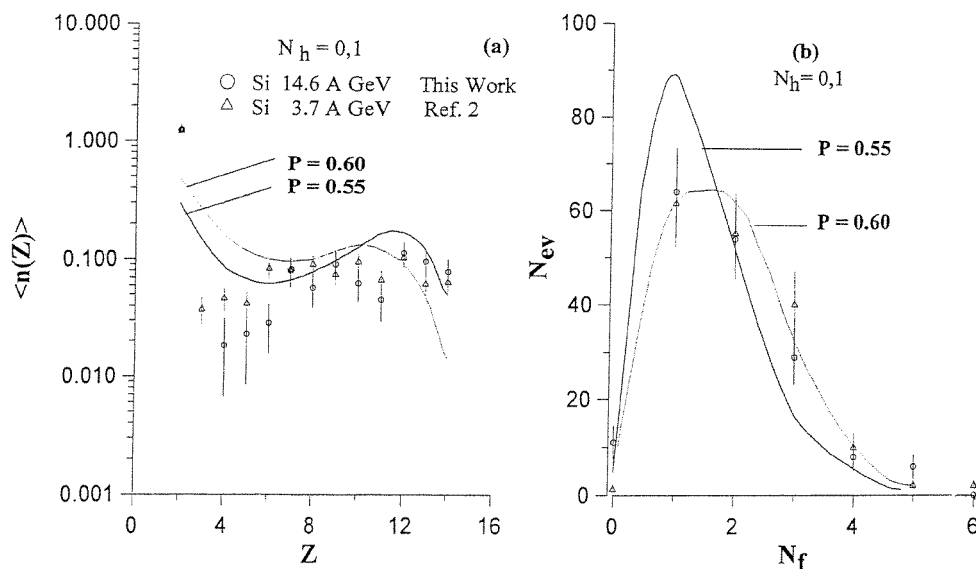
Figure 3. (*a*) Charge distribution and (*b*) multiplicity distribution of the PF in ^{28}Si interactions of quasi-nucleon type ($N_h = 0, 1$). The curves are calculated according to the bond percolation model with $P = 0.55$ and 0.60. $\langle n(Z) \rangle$ represents the frequency of charge Z, N_f is the number of PF.
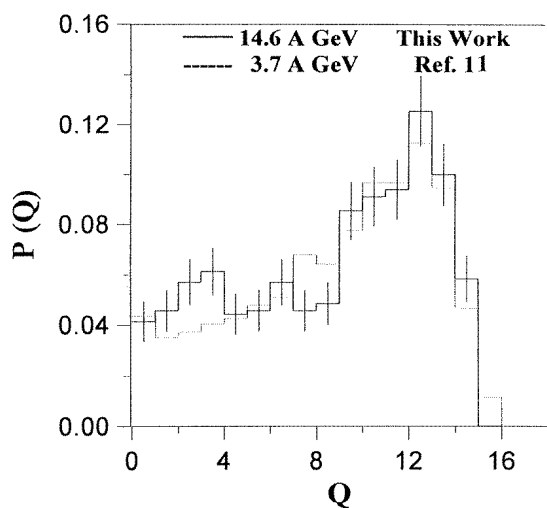

Figure 4. The overall distribution of events with a given value of Q for ^{28}Si–Em at 14.6 and 3.7 A GeV.

the break-up appears from subcritical systems on the average. Naturally, no kind of pre-formed α-substructure is introduced in the percolation simulation. The charge distribution generated by such a percolation model shows a decrease of the yield of fragments for $Z = 10$–12.

It should be noticed that the detailed description of the average charge and multiplicity distributions in figure 3 can be achieved by taking into account the dynamical effects, the impact parameter dependence of P and the later evaporation stage of fragments (see [13] for details).

It is interesting to perform the analysis of the multiplicity dependences on the quantity Q per event which measures the total charge of non-interacting PF for inelastic interaction, i.e.,
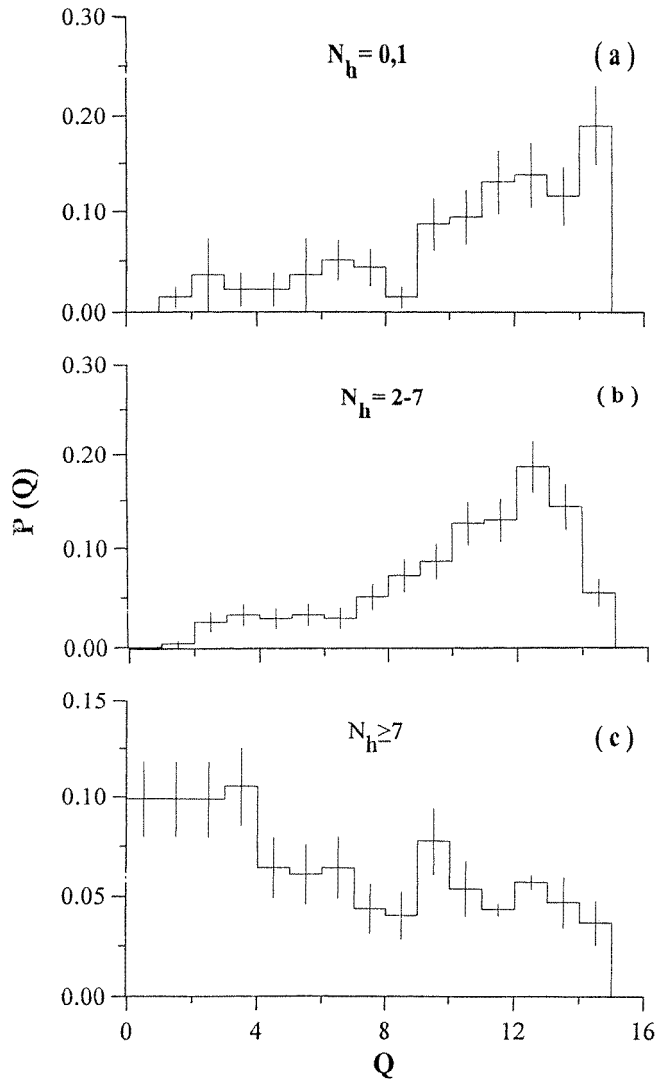
Figure 5. The distribution of events with a given value of Q: (*a*) for $N_h = 0, 1$, (*b*) for $N_h = 2$–7 and (*c*) for $N_h \geqslant 8$.

$Q = \sum_i n_i Z_i$, where n_i is the number of fragments with charge $Z_i \geqslant 1$ in an event. The value of Q characterizes the volume of the non-overlapping part of the projectile nucleus. Thus, this quantity enables us to estimate the average number of interacting nucleons per event, i.e., $N_{int} \simeq (Z_p - Q)A_p/Z_p$ where Z_p and A_p are the atomic and mass numbers of the projectile nucleus.

The distributions of events with a given value of Q for ^{28}Si–Em interactions at 14.6 A GeV (solid histogram) and 3.7 A GeV [14] (broken histogram) are shown in figure 4. It is clear that the two histograms follow the same trend. However, it can be noticed that there are some differences around $Q = 3, 4$ and $Q = 8, 9$ which may be due to statistical reasons. A similar result has been given by Adamovich *et al* [15] for 200 A GeV ^{16}O–Em interactions. It is concluded that the distributions of total charge of non-interacting PF 'Q' are independent
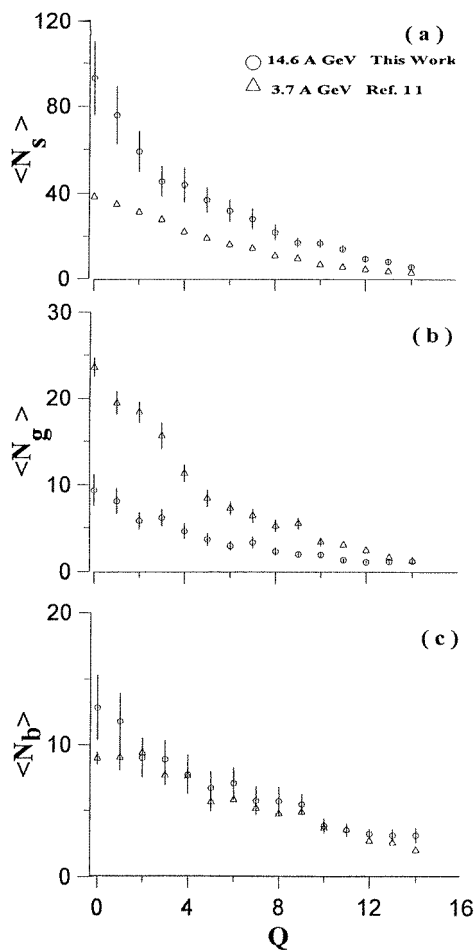
Figure 6. The average multiplicity of (*a*) shower (*b*) grey and (*c*) black track particles as a function of Q for ^{28}Si at 14.6 and 3.7 A GeV.

of energy.

Effects of impact parameter (as indicated by the value of N_h) on the total charge of the PF are displayed in figure 5 for $N_h = 0, 1$; $N_h = 2–7$ and $N_h \geqslant 8$. It can be noticed that the major contribution for quasi-nucleon events (i.e., $N_h = 0, 1$) is toward the high values of Q. In figure 5(*b*) the yield increases with the net charge of the spectators Q, which is connected with the gentle low-temperature processes, while in figure 5(*c*) the yield decreases with Q, which characterizes the violent high-temperature processes.

Figure 6 shows the normalized values for average multiplicities of shower, grey and black track particles as a function of the total charge of non-interacting PF 'Q' for the two Si beams at 14.6 A and 3.7 A GeV [14]. It is interesting to notice that the mean number of shower particles $\langle N_s \rangle$ increases with decreasing Q, and its maximum values are at $Q = 0$: i.e., when Si constituents are completely participated in the collision and a large amount of energy is transferred to the target nucleus, $\langle N_s \rangle$ increases rapidly with increasing beam energy. The variation of $\langle N_g \rangle$ and $\langle N_b \rangle$ (target fragments), as a function of the spectator projectile charge Q, are shown in figures 6(*b*) and (*c*), respectively. One can see that all values of N_g are higher for interactions at 3.7 A GeV than those at the higher energy, 14.6 A GeV. This may be due to the possible emission of high-energy grey track particles in the exposure of 14.6 A GeV

such that an overlap may occur between the limits of the specific ionization characterizing the grey and shower tracks. The multiplicities of N_g fragments increase rapidly with increasing centrality (i.e., with lower Q). This dependence is weaker in the case of black particles, which consist only of slow target fragments and the dependence of black particles on the projectile energy is weaker than that for grey particles.

4. Concluding remarks

The results obtained from this study lead to the following conclusions:

(1) The yield of multiply-charged fragments is the same for the process of ^{28}Si (14.6 and 3.7 A GeV) and ^{32}S (200 A GeV) fragmentation. This reflects the fact that the beam energy is of little importance for the nuclear fragmentation process except probably for the most peripheral interactions.

(2) The cross section of total projectile destruction events follows a geometrical formula like the one suggested by Bradt and Peters for relativistic inelastic nucleus–nucleus collisions.

(3) The multiplicity and charge distributions of fragments with $Z \geqslant 6$ are qualitatively described by a statistical percolation model for quasi-nucleon events where the size of the fragmenting system is well defined. The rise for $Z = 2$ is predicted and for $3 \leqslant Z \leqslant 5$ is not well described.

(4) The charge and multiplicity distributions for PF having $Z \geqslant 2$ in ^{28}Si-ions are similar at 14.6 A and 3.7 A GeV for all ranges of N_h.

Acknowledgment

References

[1] El-Nagdy M S 1993 *Phys. Rev.* C **47** 346
    Harris J W *et al* 1987 *Phys. Rev. Lett.* **58** 463
[2] Adamovich M I *et al* (EMU01 Collaboration) 1995 *Z. Phys.* A **351** 311
[3] El-Nadi M, El-Nagdy M S, Metwally N M, Badawy O E and Kelany L 1994 *Nuovo Cimento* A **107** 1
[4] El-Nadi M, El-Nagdy M S, Shaat E A, Abou-Mossa Z, Kamel S and Abdella A M 1997 *Int. J. Mod. Phys.* E **6** 135
[5] Powel G F *et al* 1959 *The Study of Elementary Particles by Photographic Method* (Oxford: Pergamon) p 587
[6] Price P B and He Y D 1991 *Phys. Rev.* C **43** 835
[7] Singh G, Jain P L and El-Nagdy M S 1992 *Europhys. Lett.* A **7** 113 and references therein
[8] Kalmykov N N and Ostapchenko S S 1993 *Phys. At. Nucl.* **56** 3
    Kalmykov N N and Ostapchenko S S 1993 *Phys. At. Nucl.* **56** 346
[9] Bogdanov V G *et al* 1988 *Yad. Phys.* **47** 1814
[10] Bradt H L and Peters B 1950 *Phys. Rev.* **77** 54
[11] Bauer W *et al* 1986 *Nucl. Phys.* A **452** 699
[12] Campi X 1986 *J. Phys. A: Math. Gen.* **19** 917
[13] El-Nadi M, El-Nagdy M S, Abdelsalam A, Shaat E A, Ali-Mossa N, Abou-Moussa Z, Abdel-Waged Kh, Osman W and Abdel-Wahed F A 1998 *J. Phys. G: Nucl. Part. Phys.* **24** 2265
[14] Adamovich M I *et al* 1992 *Preprint* JINR E1-92-569
[15] Adamovich M I *et al* 1989 *Phys. Lett.* B **223** 262